IEEE Access
Multidisciplinary : Rapid Review : Open Access Journal

Received 27 October 2023, accepted 29 November 2023, date of publication 5 December 2023,
date of current version 13 December 2023.

Digital Object Identifier 10.1109/ACCESS.2023.3340131

RESEARCH ARTICLE

EV Charging Profiles and Waveforms Dataset (EV-CPW) and Associated Power Quality Analysis

ISLA ZIYAT[1], (Member, IEEE), ALIA GOLA[2], PATRICK R. PALMER[1], (Senior Member, IEEE), STEPHEN MAKONIN[3], (Senior Member, IEEE), AND FRED POPOWICH[4]

[1]School of Mechatronic Systems Engineering, Simon Fraser University, Surrey, BC V3T 0A3, Canada
[2]School of Sustainable Energy Engineering, Simon Fraser University, Surrey, BC V3T 0N1, Canada
[3]School of Engineering Science, Simon Fraser University, Burnaby, BC V5A 1S6, Canada
[4]School of Computing Science, Simon Fraser University, Burnaby, BC V5A 1S6, Canada

Corresponding author: Isla Ziyat (isla_ziyat@sfu.ca)

This work was supported in part by the Natural Resources Canada (NRCan) under Project titled "Tap&Go Electric Vehicle Charging Infrastructure Demonstration" under Grant Evid-3001, and in part by the Natural Sciences and Engineering Research Council of Canada (NSERC) under Discovery Grant RGPIN-2018-06192.

ABSTRACT The rapid growth of electric vehicle (EV) charging will present challenges to electrical distribution networks and will affect grid operation and reliability. In order to improve the understanding of EV charging behaviour, we present the open access *EV Charging Profiles and Waveforms* (EV-CPW) dataset for AC charging. The dataset comprises of charging profiles and high-resolution current/voltage AC waveforms for 12 different EV's, including popular battery EV's and plug-in hybrid EV's. A power quality analysis is carried out to compare the EV charging behaviours to new standards recommendations proposed by standards agencies. This includes evaluating power factor, current and voltage distortion, harmonic content and load behaviour in relation to grid voltage and frequency. The preliminary data analysis presented reveals that each EV has distinctive charging characteristics and the power quality analysis indicates variation in the on-board charger circuits employed by the EV's. The EV-CPW dataset can be used for many more applications and studies, including EV charging infrastructure planning, demand management, EV charging coupled with renewable energy studies, power quality analysis, equipment lifetime studies and power electronics design. The dataset can be accessed at https://doi.org/10.7910/DVN/F81CXW.

INDEX TERMS Electric vehicles, dataset, EV charging, level 2 charging, power quality, AC waveforms, charging profiles.

I. INTRODUCTION

Over the last few years, there has been a noticeable increase in electric vehicles (EV's), representing a total of 14% of new car sales globally in 2022 [1], including both battery EV's (BEV's) and plug-in hybrid EV's (PHEV's). Public electric charger stock has been increasing globally by 50% each year since 2015 [1]. This surge in EV charging will directly impact distribution networks and challenge grid operation and planning.

Possible impacts from EV charging include:

- **Peak loading**: EV charging increases the loading in the grid, which could worsen the peak demand and create significant energy management challenges.
- **Network overloading**: Increased loading results in distribution lines reaching maximum current, which may require expensive line upgrades.
- **Power quality issues**: Harmonics are created due to the power electronics required for EV charging which will decrease the distribution network's power quality and could damage utility equipment and consumer loads [2].
- **Premature equipment failure**: Higher current and harmonics near EV chargers could lead to premature failure of utility transformers [3].
- **Capacity under-utilisation**: Single-phase charging, such as Level 1 and Level 2 chargers, can lead to significant phase unbalance, that can results in capacity under-utilisation when only one phase becomes overloaded [4].

The associate editor coordinating the review of this manuscript and approving it for publication was Dinesh Kumar.

Overall, these impacts could lead to reduced grid reliability and costly network upgrades reflected in higher consumer rates for everyone.

To accurately study the impact of EV charging, real data is necessary, however datasets relating to EV charging are scarce. Some datasets are generated by models such as the EVI-Pro tool [5], which includes the aggregate charging data for specific locations in the U.S. Real-world data is published in the Vehicle Energy Dataset (VED) dataset that includes fuel, energy and vehicle trajectory data for gasoline and electric vehicles [6]. Existing EV charging datasets include charging sessions of existing charger networks, such as ACN-Data for the network located at CalTech University [7] and a dataset for a large U.S. workplace in [8]. However, these datasets contain lumped energy usage for each charging session, without any EV charging profile resolution.

For EV specific behaviour, including high-resolution charging data, most researchers rely on EV charger models and simulations [9], [10], [11], [12], [13], rather than real measurement datasets. Although Slangen et. al experimentally tested nine BEV's in order to assess harmonics, the data is not published and the EV's tested are not specified [14].

To the authors' knowledge, EV charging data for specific EV's, including charging profiles and current/voltage waveforms, does not yet exist in the public domain. In this paper, the *EV Charging Profiles and Waveforms* (EV-CPW) dataset is published which contains measurement data from 12 different EV's charged on an AC Level 2 (L2) charger. This open access dataset includes 1-minute interval data for each EV's charging profiles, including real power, reactive power, RMS voltage and RMS current. Additionally, high-resolution AC current and voltage waveforms are captured hourly and are sampled at 30 kHz. The EV's tested include popular EV's in North America, including the Tesla Model 3/Y, the Hyundai Ioniq 5 and the Toyota Prius Prime.

Although developing standards exist for electric vehicle supply equipment (EVSE), these do not apply to EV's and their on-board chargers. A need for new studies is highlighted in [15], in order to recommend best practices and improve standards to help ensure bulk power system reliability, resilience, and security. In this paper, a preliminary power quality analysis of the EV-CPW dataset is carried out and compared with the recommended standards by proposed by standards agencies [15], [16].

The contributions of this paper are summarised as follows:

1) The *EV Charging Profiles and Waveforms* (EV-CPW) dataset is presented and made publicly available. It includes charging profiles and high-resolution transient current/voltage waveforms for 12 EV's.
2) A power quality analysis, including power factor, distortion, harmonic analysis, and load behaviour is carried out on the 12 EV's and compared to EV standard recommendations proposed by standards agencies.

II. DATASET USAGE

The dataset published can be used by researchers for a wide range of studies. Potential applications of the 1-minute charging profiles include but are not limited to:

- **Power flow analysis**: High time-resolution three-phase power flow can be studied to facilitate EV charger infrastructure planning. This includes grid compliance studies, and optimal siting and sizing of EV chargers [17]. This also facilitates the integration of EV chargers coupled with renewable energy sources (RES), as studied in [18] for solar PV.
- **Energy management studies**: Demand side management of EV chargers can be studied, for example smart charging algorithms for scheduling and control [19], vehicle-to-grid (V2G) techniques [20], peak shaving strategies and the impact of time-of-use pricing [2].
- **Electric mobility patterns**: By coupling EV-CPW with other existing datasets such as VED [6], and ACN-data [7], EV charging patterns alongside EV driving patterns and trajectories can be studied to assess the overall EV usage, improve the siting of EV chargers, study consumer behaviour and the impact on transportation emissions.

Potential applications for the current/voltage AC waveforms in the EV-CPW include but are not limited to:

- **Power quality analysis**: Harmonic analysis, distortion, power factor of distribution networks as a result of EV charging can be analysed. Moreover, equipment lifetime assessments can be carried out, specifically for transformers that are known to be poorly affected by harmonics [3].
- **Equipment design**: The transient waveforms can be used to study power electronics and controller design. This includes the design of on-board and off-board chargers, RES converters located near EV chargers, and converters used for grid services such as such as active power filters used to filter out harmonics.
- **EV battery lifetime assessment**: The impact that different charging profiles and on-board charger power quality has on battery health and lifetime can be analysed [21].

III. EV CHARGER TYPES

EV chargers can be categorised as either AC or DC charging. AC chargers include Level 1 (L1) and Level 2 (L2) chargers, which are single-phase connected to the grid, as seen in Fig. 1. L2 and L1 chargers are similar, but L2 chargers operate at a higher voltage than the L1 chargers, allowing for faster charging. These charger types rely on the EV's on-board charger, as seen in Fig. 1, to convert AC to the DC voltage required at the battery. In North America, the AC connector used is SAE J1772 [22] but different connectors are used in Europe and China although similar voltage ranges are used for AC charging (208-240 V) [2].

DC chargers, also known as Level 3 (L3), comprise of a AC-DC three-phase converter within the charger itself which is known as an off-board charger, as seen Fig. 1. Therefore, the grid impact due to L3 charging is dictated by the charger design, whereas for L2 charging it is dictated by the EV's on-board charger design, for which many topologies and controllers exist [21].

Both BEV's and PHEV's are compatible with AC charging, whereas a smaller fraction of EV's, typically BEV's only, can use DC charging. Level 2 charging has so far been more popular for public charging [1] which may also be due to the lower cost compared to Level 3 chargers. In this paper, the EV charging data from AC charging is collected, by charging EV's on Level 2 chargers.

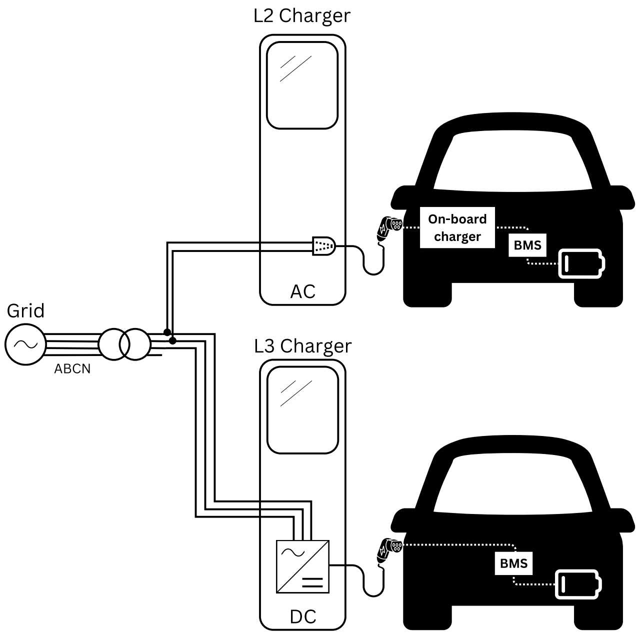

FIGURE 1. Simplified diagram of L2 and L3 charger connections. The L2 (AC) charger is a direct connection to the grid and requires an on-board charger before the battery management system (BMS).

IV. STANDARDS AND RECOMMENDATIONS

The developing standards for EV chargers include the international standard IEC 61851-1 [23] and CSA C22.2 No. 280 which is tri-national standard with NMX-J-677-ANCE and UL 2594, for Canada, U.S. and Mexico [24].

Standards required for on-board chargers tend to be customer load and small home appliances standards, for example IEEE 519 [25], IEC 61000-3-2 [26] and IEC 61000-3-12 [27]. IEC 61851-21-1 is the only on-board charger specific standard and has the same harmonic limits as the IEC 61000 series.

Standards are still developing for both on-board and off-board charging, but so far power quality standards specific to EV charging do not exist [13]. Regulatory and standards organisations have recently formed working groups in order to provide recommendations for best practices for EV charging, in order to improve the standards [15], [16]. California Mobility Center (CMC), the North American Electric Reliability Corporation (NERC) and the Western Electricity Coordinating Council (WECC) recommended "grid-friendly" EV charging behaviour [15]. Additionally, the Society of Automotive Engineers (SAE) produced a recommended practice document for power quality requirements for plug-in EV chargers [16].

A. LOAD BEHAVIOUR

Loads connected to the grid can be categorised as constant impedance, constant current, or constant power. Electronically-coupled loads, such as the power electronic converters found in chargers, tend to maintain either constant power or constant current level regardless of voltage and frequency [28]. Constant power loads exacerbate system instability because during events when the voltage reduces, the load draws more current in order to maintain constant power [15]. Moreover, if the utility requires a decrease in loading they cannot conveniently decrease the system voltage to achieve this. In contrast, constant current loads reduce in power when the system voltage decreases. The NERC/CMC/WECC working group suggests that EV chargers and EVSE's should employ a steady-state control strategy that use constant current control rather than constant power level control during normal operations [15].

Moreover, the NERC/CMC/WECC working group suggests that EV's and EVSE's should support reliability by actively contributing to the system's frequency response [15]. They recommend that EV/EVSE's should employ a control strategy to ensure that active power consumption is proportional to the frequency measured at the EV charger [15], [28].

B. HARMONICS

In the grid, the AC voltage and current waveforms should ideally be pure sinusoidal waveforms at the fundamental frequency (60 Hz). However, higher frequencies typically exist due to non-linear loading. These higher frequencies are integer multiples of the fundamental frequency and are known as harmonics [16].

1) CURRENT HARMONICS

Current harmonics are undesired, as only the fundamental frequency contributes to power delivery, whereas harmonics only result in losses such cable heat [16]. Moreover, current harmonics can lead to voltage distortion which may cause damage to other equipment and appliances connected to the grid. To assess the current harmonics, the current total harmonic distortion can be measured as,

$$THD_i = \frac{\sqrt{\sum_{h=2}^{\infty} I_h^2}}{I_1} \tag{1}$$

where I_1 is the rms of the fundamental harmonic, and I_h the rms of the harmonics. THD_i becomes high for small currents, therefore total demand distortion is more commonly used,

$$TDD = \frac{\sqrt{\sum_{h=2}^{\infty} I_h^2}}{I_L} \tag{2}$$

where I_L is the maximum circuit current.

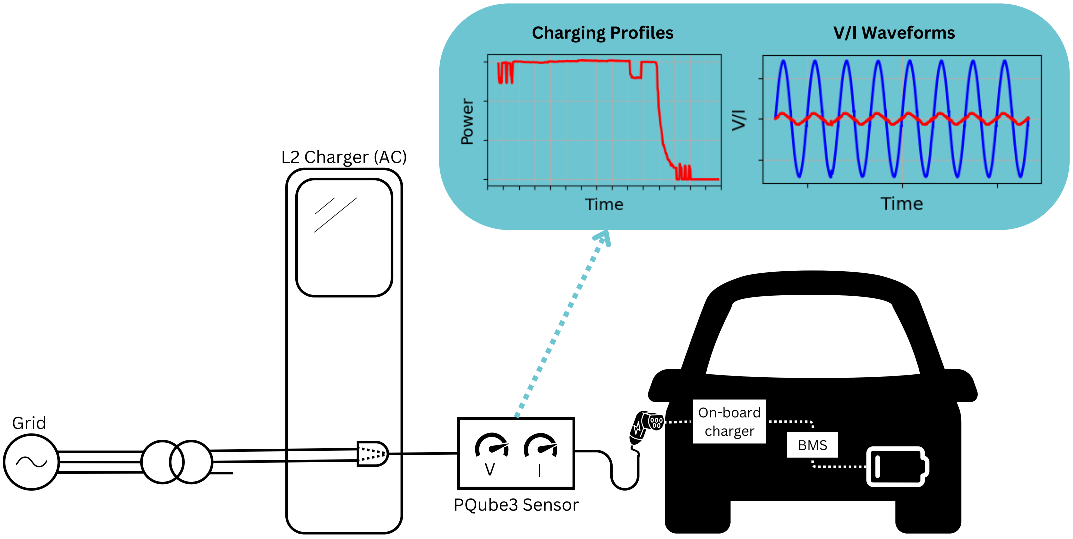

FIGURE 2. Experimental test setup diagram showing the EV connection to charger via the sensor. The sensor data collected includes charging profiles and voltage/current waveforms.

The recommended limit by the SAE for each current harmonic is outlined in Table 1, with a total TDD limit of 10% for all current ranges [16].

TABLE 1. SAE Recommended individual hamonic limits and TDD limit for AC Level 2 current ranges [16].

Harmonic Order	Limits (A) 0-16 A	Limits (A) 16-24 A	Limits (A) 24-40 A
2	0.56	0.83	1.39
3	1.19	2.25	3.76
4	0.22	0.42	0.70
5	0.59	1.12	1.86
6	0.16	0.28	0.46
7	0.40	0.75	1.25
8	0.18	0.21	0.35
9	0.21	0.40	0.66
10	0.15	0.17	0.28
11	0.17	0.32	0.54
12	0.12	0.14	0.23
13	0.11	0.21	0.35
TDD %	**10.0**	**10.0**	**10.0**

2) VOLTAGE HARMONICS

The SAE recommendation for voltage harmonics, refers to the IEEE 519 standards for utilities [16], [25]. Similarly to current distortion, total harmonic distortion for voltage is given by,

$$THD_v = \frac{\sqrt{\sum_{h=2}^{\infty} V_h^2}}{V_1} \tag{3}$$

IEEE 519 states that the THD_v should not exceed 5%, and no individual voltage harmonic should exceed 3% [25].

C. POWER FACTOR

Although reactive power control is beneficial to system stability and operation, the presence of unintended reactive power loading in distribution networks leads to higher currents and losses in the lines, and minimises the capacity for real power delivery. Therefore, restricting power factor in passive loads improves system efficiency. Power factor is calculated as,

$$PF = \frac{P}{S} \tag{4}$$

where P is real power and S apparent power.

The NERC/CMC/WECC working group suggests a power factor limit of 0.985 or higher (leading or lagging) for EV chargers [15], whereas the SAE recommendation suggests a power factor limit of 0.95 or higher [16].

TABLE 2. Properties for each EV in the EV-CPW dataset, including year, type and maximum L2 charging power.

Vehicle	Year	Type	L2 Charging (kW)
Tesla Model Y (TMY)	2022	BEV	11.0
Tesla Model 3 (TM3)	2021	BEV	11.0
Volvo XC-40 (VXC)	2021	BEV	11.0
BMW iX xDrive50 (BMW)	2023	BEV	11.0
Ford Mustang Mach E (FMM)	2022	BEV	11.0
Hyundai Ioniq 5 (HI5)	2022	BEV	11.0
Hyundai Ioniq Electric (HIE)	2017	BEV	7.2
Kia Nero EV (KNE)	2019	BEV	7.0
Lexus NX 450h+ (LNX)	2023	PHEV	7.0
Nissan Leaf SV (NL)	2019	BEV	7.0
Mitsubishi Outlander (MO)	2019	PHEV	4.0
Toyota Prius Prime (TPP)	2021	PHEV	3.0

V. DATA COLLECTION

The 12 EV's tested as part of this dataset are outlined in Table 2, alongside their properties and the abbreviation used to refer to them in the remainder of the paper. Both BEV's and

TABLE 3. Description of charging profile data provided for each EV in files called Charging_Profile.csv.

Feature	Unit	Description
Date and Time	date-time	1-minute time increment
Voltage RMS Min/Avg/Max	V	Minimum/Average/Maximum rms voltage during the 1-minute interval, measured every cycle.
Current RMS Min/Avg/Max	A	Minimum/Average/Maximum rms current during the 1-minute interval, measured every cycle.
Real Power Min/Avg/Max	kW	Minimum/Average/Maximum real power during the 1-minute interval
Reactive Power Min/Avg/Max	kVAR	Minimum/Average/Maximum reactive power during the 1-minute interval
Apparent Power Min/Avg/Max	kVA	Minimum/Average/Maximum apparent power during the 1-minute interval
Frequency Min/Avg/Max	Hz	Minimum/Average/Maximum grid frequency measured during 1-minute interval

PHEV's are tested, with varying L2 charging power dictated by their on-board chargers.

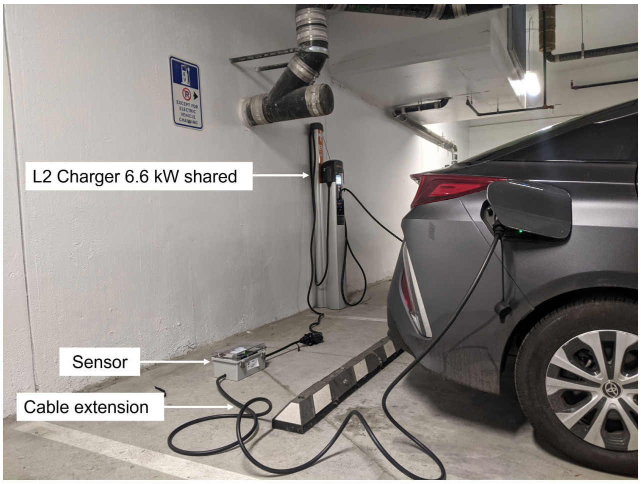

FIGURE 3. **Experimental test setup showing the L2 charger, the cable extension and sensor - Toyota Prius Prime under-test.**

During the data collection, the EV under-test is connected to a 6.6 kW Level 2 charger as seen in Fig. 2. A PQube3® AC analyzer is placed within the charger cable to measure the voltage and current into the EV. The physical test setup is seen in Fig. 3 for the Toyota Prius Prime under-test, and a close up of the sensor and extension is seen in Fig. 4.

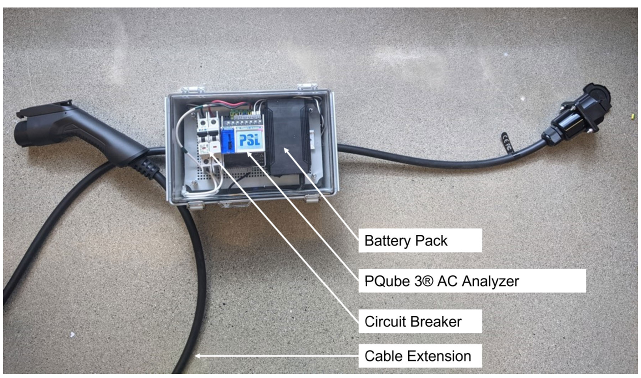

FIGURE 4. **Close up of extension cord and built-in sensor, comprising of the PQube 3 AC analyzer, a circuit breaker and a battery pack.**

The data collection mostly took place in the same location, Station A, shown in Fig. 3, over several weeks. This location is in a parking lot connected to an urban grid in Surrey, Canada. Only the Mitsubishi Outlander was tested elsewhere in a suburban grid at Station B. The two stations' parameters are outlined in Table 4.

TABLE 4. Stations' parameters.

Station	Type	Location	Power (kW)	AC Voltage (V)
A	Level 2	Urban	6.6	208-240
B	Level 2	Suburban	6.6	208-240

From the data collected by the PQube3® the EV-CPW dataset is formed comprising of:

1) The EV charging profile of each vehicle in 1-minute interval data, which includes rms voltage and current, real and reactive power and grid frequency, as seen in Table 3. The data includes the minimum, average and maximum values of these measurements during each 1-minute interval.
2) The EV high-resolution current/voltage AC waveforms are collected hourly and at a higher rate during the end-of-charge period. The waveforms include eight waveform cycles, and the current and voltage measured are sampled with 512 data points per cycle (60 Hz), hence 32.6 μs intervals. The waveform data is outlined in Table 5.

TABLE 5. Description of waveform snapshot data provided in files called Waveform_x.csv.

Feature	Unit	Description
Time	ms	Time measurement
Voltage	V	Voltage at the EV plug in
Current	A	Current into the EV

The file structure of the EV-CPW dataset is represented in Fig. 5.

VI. DATA ANALYSIS

In this section, the data collected is analysed for both the charging profiles and the waveforms, comparing the findings to the standard recommendations outlined in Section IV.

A. CHARGING PROFILES

All charging profiles include the maximum, minimum and average real power measured in each 1-minute interval, as seen for the Toyota Prius Prime in Fig. 6. The blue dots indicate the times at which the AC waveform snapshots are recorded.

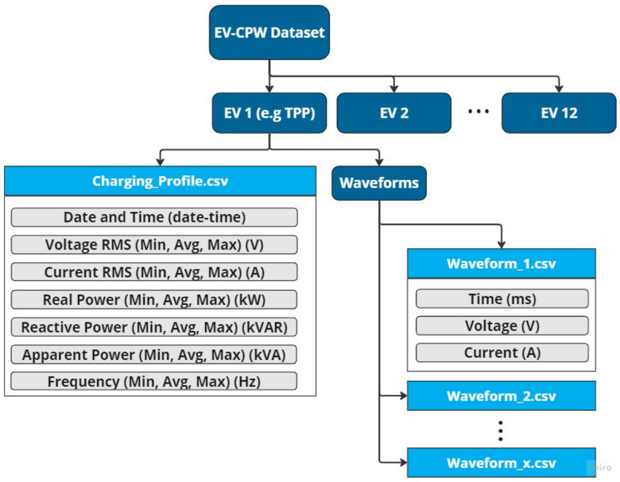

FIGURE 5. File structure of the EV-CPW Dataset.

For the Toyota Prius Prime, the real power profile is seen to regularly drop to zero, around every 15 minutes, and even more frequently at the start of charging. This same periodic turn-off behaviour is seen for the Lexus NX 450h+, in Fig. 7. Lexus is owned by Toyota, so these EV's most likely use similar on-board chargers. None of the other EV's tested had this periodic turn-off behaviour. In their end-of-charge phase, both EV's drop to a lower charging power of around 1 kW in the last 15 minutes or so of charging.

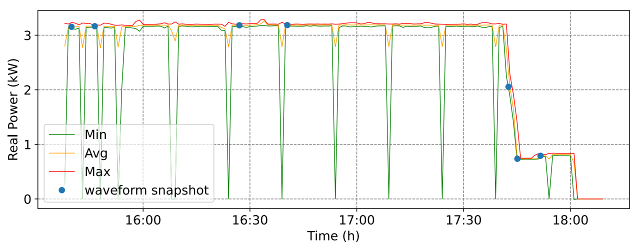

FIGURE 6. Charging Profile for the Toyota Prius Prime.

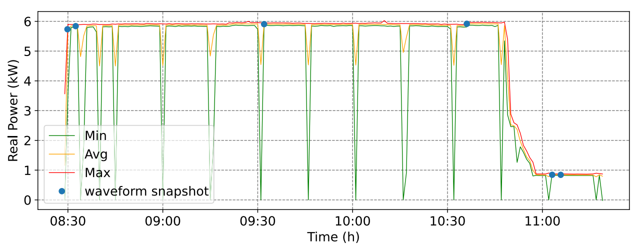

FIGURE 7. Charging Profile for the Lexus NX 450h+.

The Tesla Model Y, Fig. 8, shows constant charging behaviour but drops down to a lower charging power at 12:50 pm due to shared charging with another EV connected during that period. The Tesla Model 3, seen in Fig. 9, charged at full charger power, but drops to zero after the first 20 minutes of charging and returns to full power 5 minutes later. The Tesla Model Y and 3, did not reach full charge during the data collection, so the end-of-charge behaviours are not available.

Table 6, shows the charger station used for each charging session, the duration of each session and whether the charging stopped by the end of the session. The EV's with a lower battery capacity stopped charging indicating a full charge. However, due to the time constraint and the slower rate of charging provided by L2 charging, the EV's with high battery capacity were not fully charged by the end of testing. Due to a data accessibility constraint the state-of-charge (SOC) of each vehicle before and after the charging session is not available.

TABLE 6. Properties for each EV charging session including EV battery size, station used, duration of charging and whether or not charging stopped by the end of the charging session.

Vehicle	Battery Size (kWh)	Station Used	Charging Duration (hrs)	Charging Stopped ?
TMY	60	A	5.9	No
TM3	60	A	2.9	No
VXC	70	A	6.5	No
BMW	111	A	1.5	No
FMM	70	A	5.3	No
HI5	58	A	1.5	Yes
HIE	30	A	2.0	Yes
KNE	64	A	4.3	No
LNX	18	A	3.0	Yes
NL	40	A	7.5	Yes
MO	12	B	3.5	Yes
TPP	8.8	A	2.7	Yes

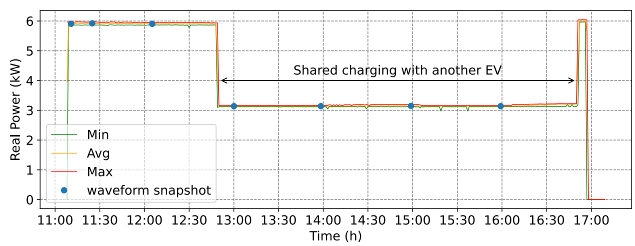

FIGURE 8. Charging Profile for the Tesla Model Y.

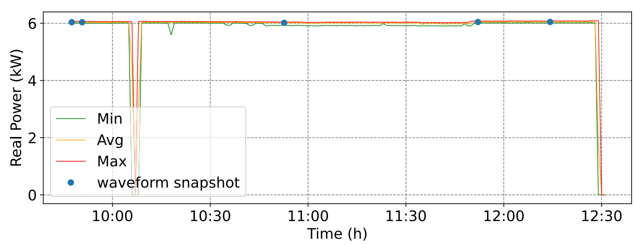

FIGURE 9. Charging Profile for the Tesla Model 3.

The Volvo XC-40, Fig. 10, shows constant charging behaviour for the first four hours of charging, but shows very unsettled behaviour for the last two hours before it is unplugged. In this second period, the real power is seen to fluctuate between maximum charger power and zero power within each 1-minute interval.

The Nissan Leaf, Fig. 11, shows a mostly constant charging behaviour, with some short sections where the power fluctuates between two levels. The end-of-charge behaviour starts at 14:00, with a smooth decrease, followed by a few pulses in the last 30 minutes.

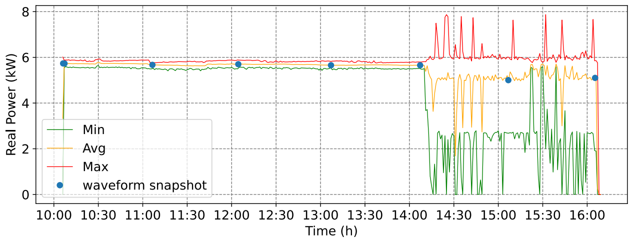

FIGURE 10. **Charging Profile for the Volvo XC-40.**

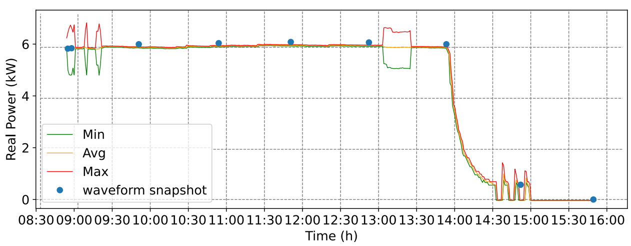

FIGURE 11. **Charging Profile for the Nissan Leaf SV.**

The Mitsubishi Outlander, Fig. 12, shows a constant charging behaviour, although the power drops to 250 W after the first 10 minutes of charging, then shortly returns to full power charging. This behaviour was repeated in subsequent charging sessions carried out to ensure that this was not an experimental error. The end-of-charge phase begins at 23:45, with a smooth decrease down to 250 W and a sharp decrease to zero.

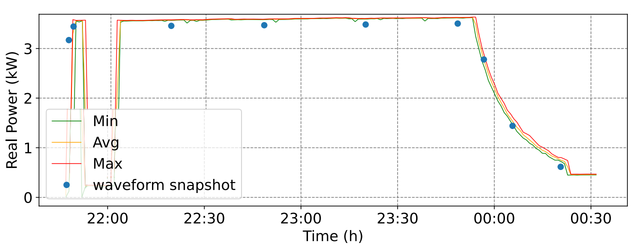

FIGURE 12. **Charging Profile for the Mitsubishi Outlander.**

The Hyundai's, Fig. 13-14, both charged at a constant rate, and reached full charge. The Hyundai Ioniq 5, Fig. 13, has a straight cut-off when fully charged unlike other EV's that gradually drop to lower powers in the end-of-charge phase.

Most EV's have a small amount of negative reactive power, i.e. capacitive loading behaviour, as seen for the Toyota Prius Prime in Fig. 15, but only the Tesla's have a positive reactive power i.e. inductive loading behaviour.

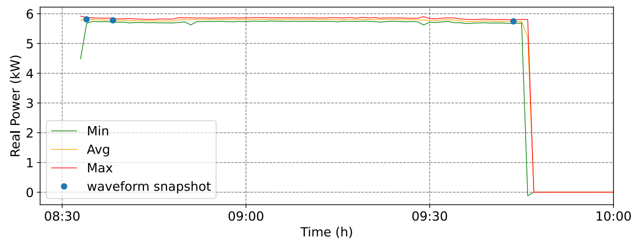

FIGURE 13. **Charging Profile for the Hyundai Ioniq 5.**

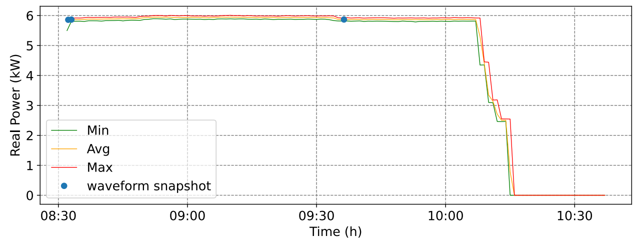

FIGURE 14. **Charging Profile for the Hyundai Ioniq Electric.**

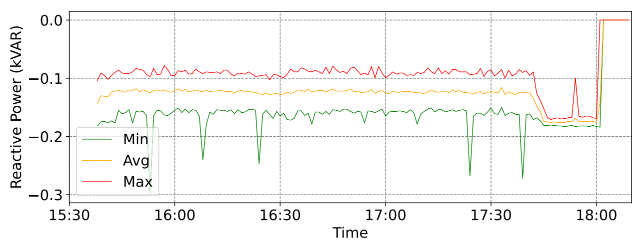

FIGURE 15. **Reactive power charging profile for the Toyota Prius Prime.**

B. VOLTAGE WAVEFORMS

The high-resolution AC voltage and current waveforms were recorded on an hourly basis, with additional snapshots used to capture the end-of-charge behaviour. The urban grid voltage (Station A), ranged from 195-210 V during all charging sessions, which is slightly lower than the expected 208-240 V required for Level 2 charging. However, this would not cause any issues for the EV charging since the minimum voltage required is 120 V as used in Level 1 chargers. An example voltage waveform, taken for the Toyota Prius Prime charging data, is shown in Fig. 16.

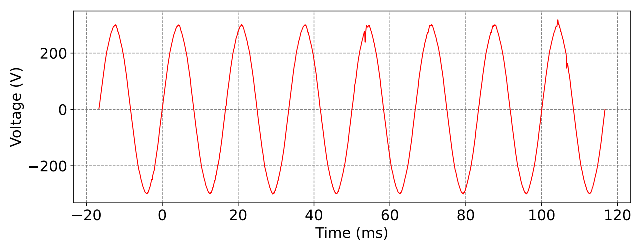

FIGURE 16. **Voltage waveform taken during the Toyota Prius Prime charging session in the urban grid.**

The Mitsubishi Outlander, however, was charged in a different location (Station B), connected to a suburban grid, which has higher voltages of around 240 V and much more distortion, as seen in Fig. 17. This is also clear from the THD_v box plot, Fig. 18, where the Mitsubishi Outlander is seen to have experienced a much worse THD_v than the other EV's. The THD_v is seen to be high for the suburban grid, even when the Mitsubishi Outlander is not charging, therefore indicating that this is a grid issue and not an issue caused by EV charging.

In Fig. 18, none of the THD_v values exceed the IEEE 519 limit of 5%. However, from the Fast-Fourier Transform (FFT) of the suburban grid, Fig. 19, it is seen that the third harmonic does exceed the 3% individual harmonic limit, imposed by IEEE 519 and recommended by SAE [16], [25]. Once more, this is a reflection on the grid's power quality rather than the effect of EV charging.

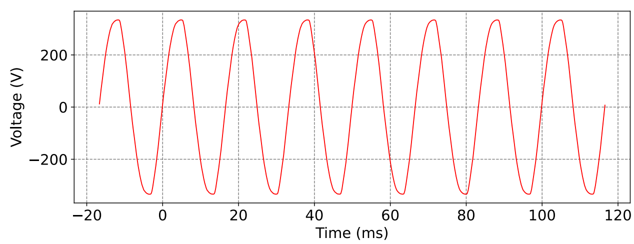

FIGURE 17. Voltage waveform taken during the Mitsubishi Outlander charging session in the suburban grid.

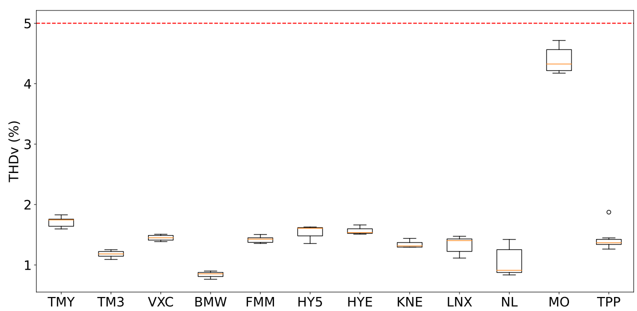

FIGURE 18. Voltage THD for all EV waveforms, in comparison to the IEEE 519 limit shown in the dashed red line.

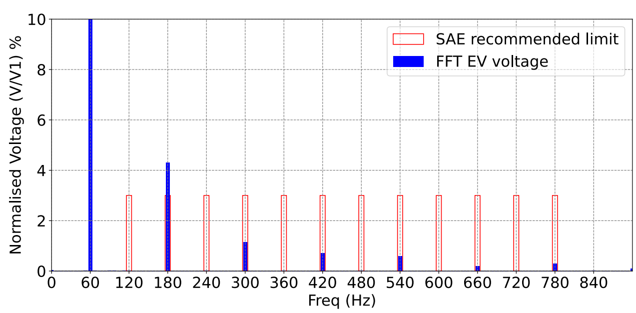

FIGURE 19. FFT of a voltage waveform from the Mitsubishi Outlander data compared to the recommended harmonic limits set by IEEE519.

C. CURRENT WAVEFORMS

The distortion in the current waveforms increases as the charging power decreases, for all the EV's, as seen in Figs. 20-24, which show higher power and lower power current waveforms. The lower power waveform snapshots are taken during the end-of-charge phase when the power reduces as it decreases to zero, and also during the reduced power phase of the Tesla Model Y.

The current waveforms greatly differ for each EV, indicating that different on-board charging circuits are used for rectification. For the Toyota Prius Prime, the third harmonic is visible in the lower current waveform, Fig. 20. For the Tesla Model Y, Fig. 21, significant distortion is visible in both higher and lower power current waveforms, including a high 7th harmonic, as well as zero-crossing distortion where the current is seen to flatten out.

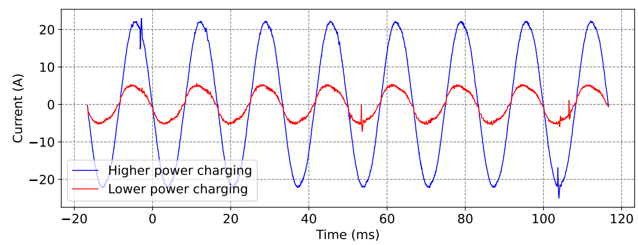

FIGURE 20. Current waveforms for higher power and lower power charging for the Toyota Prius Prime.

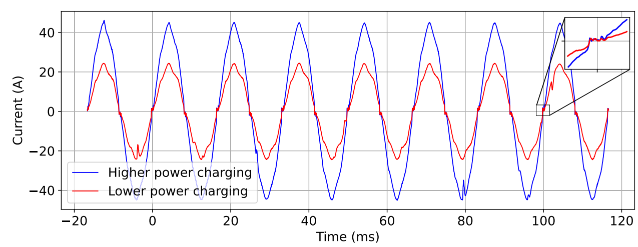

FIGURE 21. Current waveforms for higher power and lower power charging for the Tesla Model Y, with a zoom window showing the AC current zero-crossing.

The Nissan Leaf current waveforms, Fig. 22, has little distortion but some periodic notches are visible in the higher power waveform. The Lexus NX 450h+ current waveform, Fig. 23, has little distortion at higher power, however resembles a triangular wave at lower power. The Mitsubishi Outlander current waveform, Fig. 24, had the least distortion of all EV's tested.

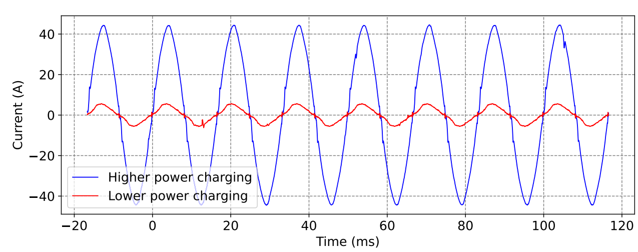

FIGURE 22. Current waveforms for higher power and lower power charging for the Nissan Leaf SV.

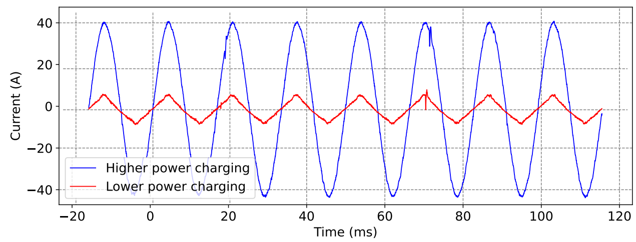

FIGURE 23. Current waveforms for higher power and lower power charging for the Lexus NX 450h+.

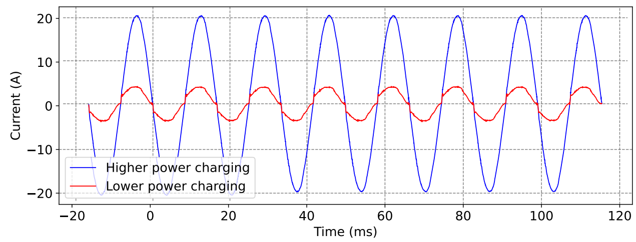

FIGURE 24. Current waveforms for higher power and lower power charging for the Mitsubishi Outlander.

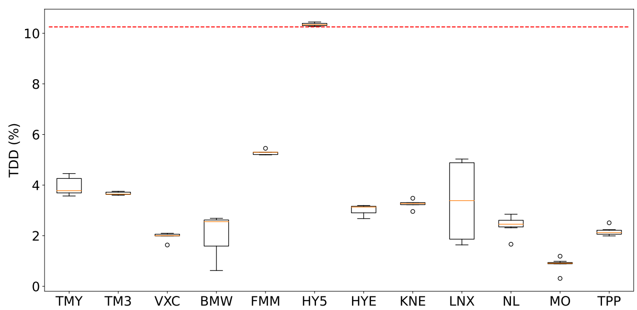

FIGURE 25. Current TDD for all EV current waveforms, in comparison to the recommended limit proposed by SAE shown in the dashed red line [16].

The *TDD* from all the current waveforms is represented in Fig. 25. This shows that all EV's are below the 10% recommended limit set by SAE [16], except for the Hyundai Ioniq 5 which has the highest *TDD*. This is reflected in its current waveforms, for example the one in Fig. 26, and its associated FFT, Fig. 27.

Despite the Mitsubishi Outlander being connected to the grid with the highest THD_v of almost 5%, it has the lowest *TDD* out of all the EV's. It has a lower charging power than the other EV's which was was taken into account in the *TDD* by setting I_L to the EV's maximum current rather than the charger's maximum current (2). In comparison to the Hyundai Ioniq 5 current FFT, Fig. 27, the current harmonics of the Mitsubishi Outlander are very small, as seen in Fig. 28.

D. POWER FACTOR

The power factor from all current/voltage waveforms of each EV is represented in a box plot in Fig. 29. Generally, all EV's are within the NERC/CMC/WECC recommended limit of 0.985 [15] and the 0.95 limit recommended by SAE [16]. Several EV's have one instance where the power factor

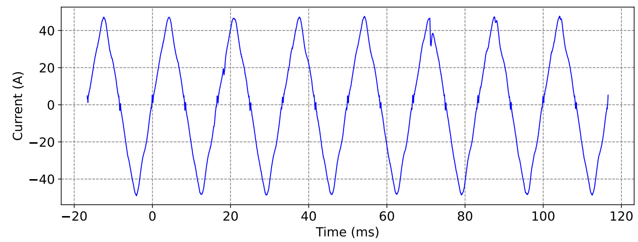

FIGURE 26. Current waveform from the Hyundai Ioniq 5.

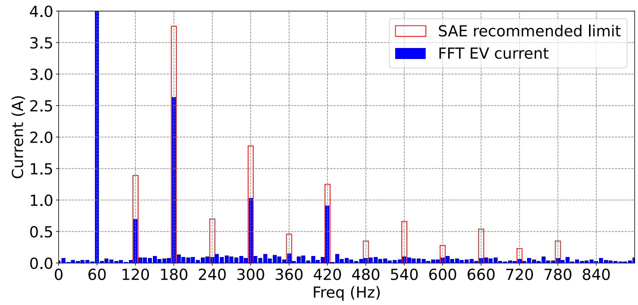

FIGURE 27. FFT of a current waveform from the Hyundai Ioniq 5, compared to the recommended harmonic limits proposed by the SAE.

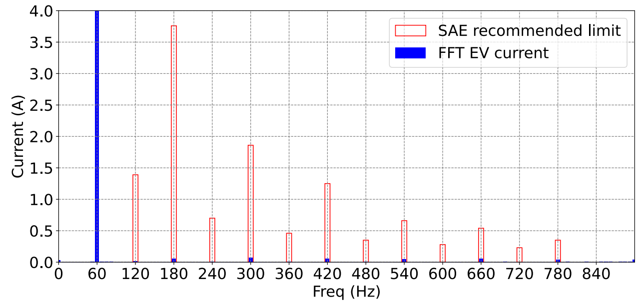

FIGURE 28. FFT of a current waveform from the Mitsubishi Outlander, compared to the recommended harmonic limits proposed by the SAE.

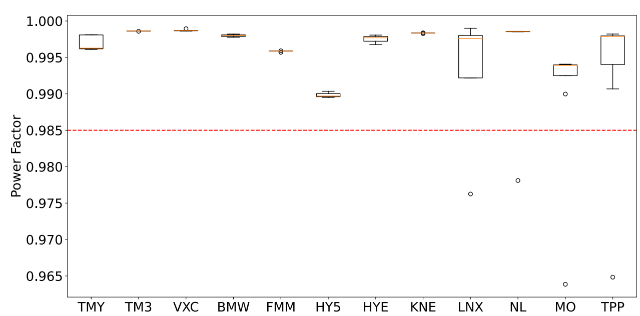

FIGURE 29. Power factor for each EV current/voltage waveforms in comparison to recommended limit proposed by NERC/CMC/WECC shown in the dashed red line [15].

is below 0.985, which occurred during their end-of-charge phase.

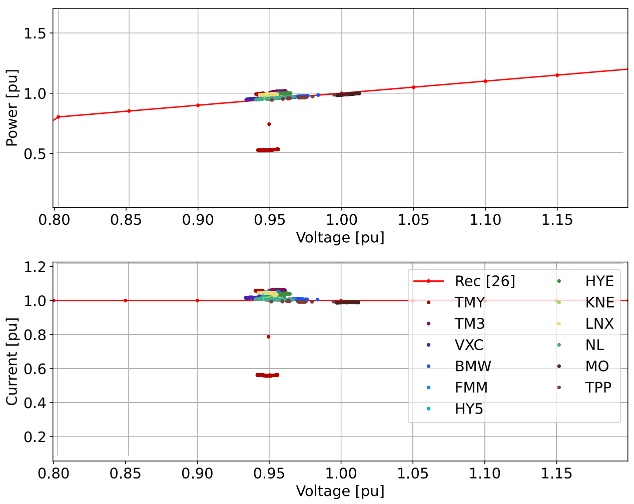

FIGURE 30. Performance curves for voltage sensitivity compared to the recommended behaviour proposed by Quint et al. [28].

E. LOAD BEHAVIOUR

As discussed in Section IV-A, it is desirable from a grid perspective for EV's to behave as constant current loads rather than constant power loads. Fig. 30 shows the power/voltage and current/voltage relationships for all the EV's. The average current, voltage and power values from the 1-minute interval data are used, filtering out the data points from the controlled end-of-charge period, and the periodic turn-off behaviours. The recommended performance curves established by Quint et al. [28], shows the recommended constant current and power behaviour, as seen in Fig. 30. Although the range of voltages for the tested EV's is narrow, the existing data shows a constant current behaviour within this range, but further data is required to conclude on the load behaviours of EV's. The few lower power data points from the Tesla Model Y are due to its lower power charging period when another EV charged next it.

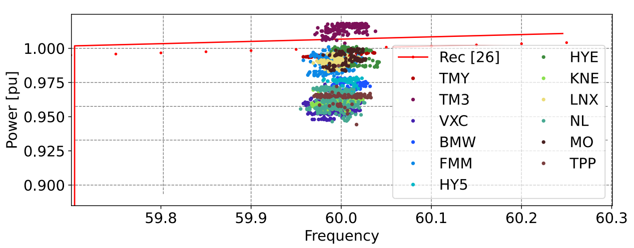

FIGURE 31. Performance curves for frequency sensitivity compared to the recommended behaviour proposed by Quint et al. [28].

For the frequency sensitivity, Fig. 31, Quint et. al recommend a frequency droop, as seen in Fig. 31. For the data collected, there seems to be no droop control present in the on-board chargers of the EV's tested, as the power varied largely in the narrow frequency range measured, as seen in Fig. 31, however a larger frequency range is needed to validate this.

VII. DISCUSSION

By comparing the EV charging data of the EV-CPW dataset, it is clear that the 12 EV's studied have greatly varying charging behaviour and power quality, indicating that there is no common consensus on on-board charger design and charging control. This increases the challenge in studying the effect of EV charging on the grid through using models and clearly demonstrates the benefits of using real measurement data.

From the EV charging profiles, seen Figs. 6-12, it is seen that different charging protocols are implemented by the different EV manufacturers. Some unexpected behaviours are observed, such as the periodic turn-off behaviours seen in the Toyota Prius Prime and Lexus NX 450h+, Fig. 6 and Fig. 7, and the fluctuating power seen in the Volvo XC-40, Fig. 10. These behaviours could lead to challenges for energy management systems (EMS) which would have to rapidly control energy flow during these short pulses. This could become even more challenging as more non-dispatchable renewable energy resources become a larger part of the power supply.

In terms of power quality, most EV's in the EV-CPW dataset were found to be within the recommended limits set by SAE and NERC/CMC/WECC [15], [16], however the combined effect of EV charging must be considered. For example, cluster charging in parking lots, may lead to superposition of harmonics and a deteriorating grid power quality. On the other hand, since the EV's are seen to produce varying harmonic content with varying phase then cluster charging may actually lead to cancelling out of harmonics and a smoothing behaviour. Due to the variable nature of EV charging, remedying variable power quality issues may require dedicated equipment such as active power filters to filter out the harmonics [29].

Moreover, Level 2 charging is single-phase charging, which can lead to significant levels of phase unbalance [18], specifically in the case of cluster charging. Having access to real charging profiles facilitates the grid analysis of phase unbalance at higher resolution. Based on such studies, dedicated equipment to tackle phase unbalance may be required such as power redistributing converters [30], [31].

EV charging is predicted to increase the loading of the grid, and therefore various methods of peak shaving are being explored such as V2G, time-of-use pricing and even smart charging algorithms which restrict the flow of power through the EV chargers. It was seen in the EV-CPW current waveforms, that reduced power leads to increased current distortion. Although *TDD* decreases at lower powers, since the charging current is lower, the combined currents in a cluster charging setup could lead to significant current harmonics through the utility transformer. Therefore, restricting power through EV chargers may lead to a trade-off between loading and power quality, and also may become a frustration to EV owners who prefer to charge at full power. The relationship between power quality and charging current is also observed in [14].

VIII. CONCLUSION

To improve the understanding of EV charging behaviour, the open access EV-CPW dataset for AC charging is published, comprising of charging profiles and current/voltage waveforms for 12 different EV's. From the charging profiles, a wide variation in charging behaviour is observed, with unexpected periodic turn-off pulses for the Toyota Prius Prime and Lexus NX 450h+, and rapid power fluctuations in the Volvo XC-40.

The AC current waveforms reveal variations in harmonic content, distortion and general waveform shape, indicating variations in on-board charger circuit and control designs. The power quality analysis and comparison to recent standards recommendations, shows that all EV's remain within the 10% TDD limit, except from the Hyundai Ioniq 5. The power factor recommended limit of 0.985 is met by all EV's, however it is seen to be violated in the lower charging powers, such as the end-of-charge phase, where the current distortion is also seen to increase.

This preliminary power quality analysis reveals important insights into the EV charging behaviour. The EV-CPW dataset can be used for many more applications and studies, by researchers and industry alike, in order to guide the electrification of transportation without compromising the reliability and operation of the grid.

IX. DOWNLOADING EV-CPW

EV-CPW is a free publicly available dataset, available in the Harvard Dataverse: https://doi.org/10.7910/DVN/F81CXW

ACKNOWLEDGMENT

The authors would like to thank the EV owners that offered their EV's for the data collection.

REFERENCES

[1] International Energy Agency. (2023). *Global EV Outlook 2023*. [Online]. Available: https://www.iea.org/reports/global-ev-outlook-2023
[2] A. Dubey and S. Santoso, "Electric vehicle charging on residential distribution systems: Impacts and mitigations," *IEEE Access*, vol. 3, pp. 1871–1893, 2015.
[3] J. C. Gomez and M. M. Morcos, "Impact of EV battery chargers on the power quality of distribution systems," *IEEE Trans. Power Del.*, vol. 18, no. 3, pp. 975–981, Jul. 2003.
[4] K. Ma, R. Li, I. Hernando-Gil, and F. Li, "Quantification of additional reinforcement cost from severe three-phase imbalance," *IEEE Trans. Power Syst.*, vol. 32, no. 5, pp. 4143–4144, Sep. 2017.
[5] D.-Y. Lee, N. Reinicke, E. Wood, Y. Ge, and E. Burrell. (2021). *Electric Vehicle Infrastructure Projection Tool (EVI-Pro)*. [Online]. Available: https://www.osti.gov/biblio/1764904
[6] G. Oh, D. J. Leblanc, and H. Peng, "Vehicle energy dataset (VED), a large-scale dataset for vehicle energy consumption research," *IEEE Trans. Intell. Transp. Syst.*, vol. 23, no. 4, pp. 3302–3312, Apr. 2022.
[7] Z. J. Lee, T. Li, and S. H. Low, "ACN-Data: Analysis and applications of an open EV charging dataset," in *Proc. 10th ACM Int. Conf. Future Energy Syst.*, 2019, pp. 139–149.
[8] O. I. Asensio, M. C. Lawson, and C. Z. Apablaza, "Electric vehicle charging stations in the workplace with high-resolution data from casual and habitual users," *Sci. Data*, vol. 8, no. 1, pp. 1–7, Jul. 2021, doi: 10.1038/s41597-021-00956-1.
[9] C. Jiang, R. Torquato, D. Salles, and W. Xu, "Method to assess the power-quality impact of plug-in electric vehicles," *IEEE Trans. Power Del.*, vol. 29, no. 2, pp. 958–965, Apr. 2014.
[10] M. Falahi, H.-M. Chou, M. Ehsani, L. Xie, and K. L. Butler-Purry, "Potential power quality benefits of electric vehicles," *IEEE Trans. Sustain. Energy*, vol. 4, no. 4, pp. 1016–1023, Oct. 2013.
[11] M. Sabarimuthu, N. Senthilnathan, A. M. Monnisha, V. Kamaleshkumar, S. Krithika Sree, and P. Mala Sundari, "Measurement and analysis of power quality issues due to electric vehicle charger," *IOP Conf. Ser., Mater. Sci. Eng.*, vol. 1055, no. 1, Feb. 2021, Art. no. 012131.
[12] A. K. Karmaker, S. Roy, and Md. R. Ahmed, "Analysis of the impact of electric vehicle charging station on power quality issues," in *Proc. Int. Conf. Electr., Comput. Commun. Eng. (ECCE)*, Feb. 2019, pp. 1–6.
[13] Z. Qin, L. Wang, and P. Bauer, "Review on power quality issues in EV charging," in *Proc. IEEE 20th Int. Power Electron. Motion Control Conf. (PEMC)*, Sep. 2022, pp. 360–366.
[14] T. M. H. Slangen, T. van Wijk, V. Cuk, and J. F. G. Cobben, "The harmonic and supraharmonic emission of battery electric vehicles in The Netherlands," in *Proc. Int. Conf. Smart Energy Syst. Technol. (SEST)*, Sep. 2020, pp. 1–6.
[15] *Electric Vehicle Dynamic Charging Performance Characteristics during Bulk Power System Disturbances*, NERC, CMC, and WECC, Abuja, Nigeria, 2023, pp. 1–16.
[16] *Surface Vehicle Recommended Practice*, SAE Standard 4970-724, SAE International, Warrendale, PA, USA, 2018, pp. 1–5.
[17] Z. Liu, F. Wen, and G. Ledwich, "Optimal planning of electric-vehicle charging stations in distribution systems," *IEEE Trans. Power Del.*, vol. 28, no. 1, pp. 102–110, Jan. 2013.
[18] S. Weckx and J. Driesen, "Load balancing with EV chargers and PV inverters in unbalanced distribution grids," *IEEE Trans. Sustain. Energy*, vol. 6, no. 2, pp. 635–643, Apr. 2015.
[19] S. Martinenas, K. Knezovic, and M. Marinelli, "Management of power quality issues in low voltage networks using electric vehicles: Experimental validation," *IEEE Trans. Power Del.*, vol. 32, no. 2, pp. 971–979, Apr. 2017.
[20] M. Yilmaz and P. T. Krein, "Review of the impact of vehicle-to-grid technologies on distribution systems and utility interfaces," *IEEE Trans. Power Electron.*, vol. 28, no. 12, pp. 5673–5689, Dec. 2013.
[21] M. Yilmaz and P. T. Krein, "Review of battery charger topologies, charging power levels, and infrastructure for plug-in electric and hybrid vehicles," *IEEE Trans. Power Electron.*, vol. 28, no. 5, pp. 2151–2169, May 2013.
[22] *SAE Electric Vehicle and Plug in Hybrid Electric Vehicle Conductive Charge Coupler*, SAE International, Warrendale, PA, USA, 2017.
[23] *Electric Vehicle Conductive Charging System—Part 1: General Requirements*, IEC Standard 61851-1 Ed. 3.0, 2017.
[24] *Electric Vehicle Supply Equipment (Tri-National Standard, with UL 2594 and NMX-J-677-ANCE-2013)*, CSA Standard C22.2 280, 2022.
[25] *IEEE Standard for Harmonic Control in Electric Power Systems*, IEEE Standard 519-2022, Revision of IEEE Standard 519-2014, 2022, pp. 1–31.
[26] *Electromagnetic Compatibility (EMC)—Part 3–2: Limits—Limits for Harmonic Current Emissions (Equipment Input Current 16 A per Phase)*, IEC Standard 61000-3-2, 2020.
[27] *Electromagnetic Compatibility (EMC)—Part 3–12: Limits—Limits for Harmonic Currents Produced by Equipment Connected to Public Low-Voltage Systems with Input Current >16 A and <75 A per Phase*, IEC Standard 61000-3-12, 2021.
[28] R. Quint, D. Kosterev, J. Undrill, J. Eto, R. Bravo, and J. Wen, "Power quality requirements for electric vehicle chargers: Bulk power system perspective," in *Proc. IEEE Power Energy Soc. Gen. Meeting (PESGM)*, Jul. 2016, pp. 1–5.
[29] D. Çelik, H. Ahmed, and M. E. Meral, "Kalman filter-based super-twisting sliding mode control of shunt active power filter for electric vehicle charging station applications," *IEEE Trans. Power Del.*, vol. 38, no. 2, pp. 1097–1107, Apr. 2023.
[30] M. Stecca, T. B. Soeiro, A. K. Iyer, P. Bauer, and P. Palensky, "Battery storage system as power unbalance redistributor in distribution grids based on three legs four wire voltage source converter," *IEEE J. Emerg. Sel. Topics Power Electron.*, vol. 10, no. 6, pp. 7601–7614, Dec. 2022.
[31] I. Ziyat, J. Wang, and P. Palmer, "Voltage ripple model and capacitor sizing for the three-phase four-wire converter used for power redistribution," *IEEE J. Emerg. Sel. Topics Power Electron.*, early access, doi: 10.1109/JESTPE.2023.3289485.

ISLA ZIYAT (Member, IEEE) received the M.Eng. degree in electrical and control engineering from the University of Cambridge, in 2018. She is currently pursuing the Ph.D. degree in power electronics and power systems with the School of Mechatronic Systems Engineering, Simon Fraser University, Surrey, BC, Canada. Her research interests include power systems and smart grids, with a focus on power electronics for distribution grid services.

ALIA GOLA is currently pursuing the B.A.Sc. degree in sustainable energy engineering with Simon Fraser University, Surrey, BC, Canada. She is a Research Assistant with a focus on power electronics design for electric vehicle charging.

PATRICK R. PALMER (Senior Member, IEEE) received the B.Sc. and Ph.D. degrees in electrical engineering from Imperial College London, London, U.K. He spent more than 30 years with the Department of Engineering, University of Cambridge, Cambridge, U.K., where his research was mainly concerned with the characterization and application of power semiconductor devices, computer simulation, and circuits, with solar photovoltaic (PV) being a long-term interest. He has further interests in the simulation and optimization of hybrid propulsion systems for ships and in fully integrated SMPS design for energy-efficient digital circuits, with IEEE articles cited by Intel and Qualcomm. He joined the School of Mechatronic Systems Engineering, Simon Fraser University, Surrey, BC, Canada, in 2019. He is an Emeritus Fellow of the St. Catharine's College, University of Cambridge. He also taught at UBC, Vancouver, BC, Canada, and the University of South Carolina, Columbia, SC, USA, and has a number of patents. He founded two successful companies, the most recent being Amantys, which raised more than U.S. $10 million in funding. He is a C.Eng. in the U.K. and a P.Eng. in Canada.

STEPHEN MAKONIN (Senior Member, IEEE) received the Ph.D. degree in computing science in the area of computational sustainability from Simon Fraser University, in 2014. He has been a Software Engineer for over 24 years, working for various local/international industry clients. He is currently an Adjunct Professor of engineering science with the SFU's Big Data Hub, Simon Fraser University. He is an expert in data science, software engineering, and machine learning. His research interests include computational sustainability and understanding socioeconomic issues about technological advancement. He is with the IEEE DataPort Advisory Committee. In 2021, he became a Voting Member of the Big Data Governance and Metadata Management (BDGMM, P2957), a new standard being developed by the IEEE Standards Association (IEEE SA) and NIST. He is the Editor-in-Chief of the IEEE DataPort Metadata Review Board and an Editorial Board Member of *Scientific Data* (Nature). He is a registered Professional Engineer (P.Eng.) with Engineers and Geoscientists BC.

FRED POPOWICH received the Ph.D. degree in artificial intelligence and cognitive science from The University of Edinburgh, in 1989. Since 1989, he has been a Professor with the School of Computing Science, Simon Fraser University (SFU). His research is concerned with how computers can be used to understand human interaction, either to make it easier for human beings to interact with computers, or to make it easier for human beings to interact with each other. As such, he has been concerned with how knowledge about the world can be represented, maintained, and learned by computers. He is currently the Scientific Director of SFU's Big Data Hub, where he collaborates with researchers, partners, and communities to collect, analyze, and translate diverse data into insight, and, ultimately, into action that solves real-world problems. His contribution and outstanding service to the Canadian Artificial Intelligence Community was recognized as he became the tenth person to receive the Distinguished Service Award from the Canadian Artificial Intelligence Association (CAIAC), in 2017.